Since January 2020 Elsevier has created a COVID-19 resource centre with free information in English and Mandarin on the novel coronavirus COVID-19. The COVID-19 resource centre is hosted on Elsevier Connect, the company's public news and information website.

Food and Chemical Toxicology 133 (2019) 110758

Contents lists available at ScienceDirect

Food and Chemical Toxicology

journal homepage: www.elsevier.com/locate/foodchemtox

Discovery of Keap1 – Nrf2 small – molecule inhibitors from phytochemicals based on molecular docking

Maiquan Li[a,b,1], Weisu Huang[c,1], Fan Jie[a], Mengmeng Wang[a], Yongheng Zhong[a], Qi Chen[a], Baiyi Lu[a,*]

[a] National Engineering Laboratory of Intelligent Food Technology and Equipment, Key Laboratory for Agro – Products Postharvest Handling of Ministry of Agriculture, Key Laboratory for Agro – Products Nutritional Evaluation of Ministry of Agriculture, Zhejiang Key Laboratory for Agro – Food Processing, Fuli Institute of Food Science, College of Biosystems Engineering and Food Science, Zhejiang University, Hangzhou, 310058, China
[b] College of Food Science and Technology, Hunan Agricultural University, Changsha, 410208, China
[c] Zhejiang Economic & Trade Polytechnic, Department of Applied Technology, Hangzhou, 310018, China

ARTICLE INFO

Keywords:
Antioxidant
3D – QSAR CoMFA
Phytochemicals
Keap1 – Nrf2
Molecular docking

ABSTRACT

Various phytochemicals have been reported to protect against oxidative stress. However, the mechanism underlying has not been systematically evaluated, which limited their application in disease treatment. Nuclear factor erythroid 2 – related factor 2 (Nrf2), a central transcription factor in oxidative stress response related to numerous diseases, is activated after dissociating from the cytoskeleton – anchored Kelch – like ECH – associated protein 1 (Keap1). The Keap1–Nrf2 protein–protein interaction has become an important drug target. This study was designed to clarify whether antioxidantive phytochemicals inhibit the Keap1–Nrf2 protein–protein interaction and activate the Nrf2-ARE signaling pathway efficiently. Molecular docking and 3D – QSAR were applied to evaluate the interaction effects between 178 antioxidant phytochemicals and the Nrf2 binding site in Keap1. The Nrf2 activation effect was tested on a H_2O_2 – induced oxidative – injured cell model. Results showed that the 178 phytochemicals could be divided into high –, medium –, and low – total – score groups depending on their binding affinity with Keap1, and the high – total – score group consisted of 24 compounds with abundant oxygen or glycosides. Meanwhile, these compounds could bind with key amino acids in the structure of the Keap1 – Nrf2 interface. Compounds from high – total – score group show effective activation effects on Nrf2. In conclusion, phytochemicals showed high binding affinity with Keap1 are promising new Nrf2 activators.

1. Introduction

Oxidative stress, which is caused by an imbalance between reactive species and antioxidative stress defense systems in cells, plays a key role in many diseases, including cancers (Reuter et al., 2010), cardiovascular diseases (Anatoliotakis et al., 2013), neurodegenerative diseases (Emerit et al., 2004) et al. The nuclear factor erythroid 2 – related factor 2 (Nrf2) pathway is the major pathway that responds to reactive species and redox potentials, and Nrf2 activation is a key defense mechanism against oxidative stress (H et al., 2012). However, under physiological conditions, repressor Kelch – like ECH – associated protein 1 (Keap1) holds Nrf2 in the cytoplasm and promotes its ubiquitination (Mcmahon et al., 2003). By contrast, under pathological conditions, Nrf2 is released from Keap1, translocates to the nucleus, and triggers the transcriptional activation of ARE – dependent genes and antioxidative enzymes (Dhakshinamoorthy and Jaiswal, 2001). Thus, targeting the Nrf2–ARE signaling pathway is a logical strategy to discover therapeutic agents for diseases and conditions induced by oxidative stress. The direct inhibition of the Keap1–Nrf2 protein–protein interaction is an alternative for the discovery of small – molecule Nrf2 activators (Magesh et al., 2012). Compounds that interact with Keap1 and occupy the Nrf2 binding site in the protein can cause the dissociation of Keap1 from Nrf2 and finally induce the transcriptional activation of Nrf2 (Pang et al., 2016).

Phytochemicals have significantly contributed to drug discovery. Many studies have shown that phytochemicals in edible flowers, vegetables, and fruits prevent or mitigate chronic diseases in humans (Kumar et al., 2012; Steinmetz and Potter, 1996). Studies in the last few decades have demonstrated the benefits of phytochemicals counteracting oxidative stress. Phenolic compounds as primary antioxidants

* Corresponding author. College of Biosystems Engineering & Food Science, Zhejiang University, Hangzhou, China.
E-mail address: bylu@zju.edu.cn (B. Lu).
[1] Maiquan Li and Weisu Huang contributed equally to this work and should be considered co-first authors.

https://doi.org/10.1016/j.fct.2019.110758
Received 7 March 2019; Received in revised form 27 June 2019; Accepted 10 August 2019
Available online 11 August 2019
0278-6915/

Abbreviations

αT	α − Tocopherol
API	Apigenin
C3S	Cyanidin 3 − sambubioside
CoMFA	Comparative molecular field analysis
COP	Coptisine
EA	Ellagic acid
ECH	Echinacoside
KAEM	Kaempferol
Keap1	Kelch − like ECH − associated protein 1
L5G	Luteolin − 5 − O − glucoside
MAG	Magnoflorine
Nrf2	Nuclear factor erythroid 2 − related factor 2
PIP	Piperine
PLS	Partial least squares
QSAR	Quantitative structure–activity relationship
RUT	Rutin

can scavenge free radicals, thereby delaying or inhibiting the initiation step and interrupting the propagation step of lipid oxidation (Kiokias et al., 2008). Vitamin E functions as a peroxyl radical − scavenging antioxidant and as an inhibitor of lipid peroxidation *in vitro* and *in vivo* (Niki, 2014). Carotenoids can act as chemical quenchers undergoing irreversible oxygenation. Epidemiological studies and clinical trials showed that adequate carotenoid supplementation may significantly reduce the risk of several disorders mediated by reactive oxygen species (Fiedor and Burda, 2014). Natural alkaloids are effective under oxidative stress in DPPH, FRAP, and TEAC assays (Rehman and Khan, 2017). Some of these natural compounds exhibit antioxidant effects through activating the Nrf2 pathway; however, details on this finding are few.

Molecular docking is widely used to predict the conformation of small − molecule ligands within the appropriate target binding site accurately (Meng et al., 2011). Quantitative structure–activity relationship (QSAR) modeling is a well − used computer − aided drug design method because it can amalgamate statistics and computational chemistry as well as complement the experimental approach. Comparative molecular field analysis (CoMFA) (Cramer et al., 1988), which is a useful method in ligand − based drug design strategy, holds that appropriate sampling of steric and electrostatic fields around molecules provides information necessary for understanding their biological activities. Statistics is computed by partial least squares (PLS) regression analysis.

In this study, molecular docking and 3D − QSAR were applied to evaluate the interaction effects between 178 phytochemicals and the Nrf2 binding site in Keap1. Phenylethanoid glycosides showed better effects than other compounds. To verify the presumptive model above, 11 compounds from high −, medium −, and low − total − score groups were further studied on a H_2O_2 − induced oxidative − injured cell model, and compounds from different groups showed significantly different activation effects on Nrf2.

2. Material and methods

2.1. Search for small molecules

A search for phytochemicals was carried out using PubMed, Web of science, and Google Scholar. Keywords used for the search were “antioxidant” and “Nrf2 activators.” Natural antioxidants were selected artificially according to the classification standard of phytochemicals. Then the 3D conformer of these phytochemicals were searched in PubChem. A compound library of 178 phytochemicals, whose 3D conformer could be found in PubChem, was created (Supplement Table 1).

2.2. Chemical compounds and reagents

Cyanidin 3 − sambubioside (C3S; CAS no. 33012 − 73 − 6), luteolin − 5 − O − glucoside (L5G; CAS no. 20344 − 46 − 1), rutin (RUT; CAS no. 153 − 18 − 4), echinacoside (ECH; CAS no. 82854 − 37 − 3), apigenin (API; CAS no. 520 − 36 − 5), kaempferol (KAEM; 520 − 18 − 3), coptisine (COP; CAS no. 3486 − 66 − 6), magnoflorine (MAG; CAS no. 2141 − 09 − 5), and piperine (PIP; CAS no. 94 − 62 − 2) were purchased from Yuanye Biotechnology Company (Shanghai, China). α − Tocopherol (αT; CAS no. 10191 − 41 − 0), ellagic acid (EA; CAS no. 476 − 66 − 4), and H_2O_2 were obtained from Aladdin® (Shanghai, China). RPMI − 1640 medium and fetal bovine serum were procured from Hyclone (Logan, Utah, USA), 0.5% trypsin EDTA, penicillin, and streptomycin were purchased from Keyi (Hangzhou, China). Antibodies to Nrf2, histone H3, and β − actin; anti − mouse − horseradish peroxide (HRP) IgG; and anti − rabbit–HRP–IgG were acquired from Abcam (London, UK). α − Tocopherol was used as a positive control.

2.3. Protein and ligand structure preparation

Keap1 3D structure (Protein Data Bank (PDB) codes: 4l7b) was obtained from PDB and prepared with SYBYL X 2.0 (Ji et al., 2015). A total of 178 phytochemicals that were proven to have good antioxidant properties were selected and prepared in accordance with the procedure in Section 2.1. The SDF formats of their 3D structures were obtained from PubChem chemical library.

2.4. Docking calculations

The semi − flexible docking of natural compounds as ligands for Keap1 structures was evaluated using SYBYL X2.0. Surflex–Dock module of SYBYL is a molecular docking unit that performs flexible alignments. The results are presented as docking accuracy and screening utility (Ferreira et al., 2015). The docking procedure was started with protomol generation using a ligand − based approach. For each protein–ligand pair, three top − ranked docked solutions were saved.

Table 1
Molecular docking results of different kinds of compounds with Keap1.

Classification	Average Total_Score
Phenylethanoid glycosides	7.3113
Tocopherols	6.2478
Flavones	5.0257
Flavanols	4.9119
Anthocyanins	4.8552
Flavonols	4.7565
Stibenes	4.5216
Flavanones	4.3529
Chalcones	4.3034
Carotenoids	3.9153
Isoflavonoids	3.4539
Phenolic acids	3.3291
Quinones	3.2318
Coumarins	3.1289
Terpenes	3.0130
Alkaloids	2.5660
Organosulfurs	1.9453
Others	1.8592

2.5. 3D − QSAR (CoMFA) studies

In consideration that the results of CoMFA studies are sensitive to the alignment of molecules, the alignment of 3D structures plays a vital role during CoMFA analysis. The lowest energy conformer of analog was chosen as a template structure for the molecular alignment of the data set. Molecules in their respective lowest energy conformations were superimposed on the template using the rigid − body fit option in SYBYL − X 2.0 (Singh et al., 2007). Following the standard procedure, SYBYL − X 2.0 was used to create a database of 178 phytochemicals. The PLS algorithm was used to obtain the relationship between the structural parameters and the binding affinity. Cross − validation analysis was performed using the leave − one − out method, wherein 20 compounds were removed from the dataset and their activity were predicted using the model derived from the rest of the dataset. The cross − validated R2 that resulted in the optimum number of components and lowest standard error of prediction was selected (Zhang and Zhong, 2010).

2.6. Cell culture

Rat adrenal pheochromocytoma line (PC12 cells) was obtained from the Institute of Biochemistry and Cell Biology, SIBS (CAS, Shanghai, China). The cells were maintained in RPMI − 1640 (Hyclone) containing 10% fetal bovine serum (Hyclone), 100 U/mL penicillin, and 0.1 mg/mL streptomycin at 37 °C with 5% CO2. The medium was changed every other day.

PC12 cells were seeded in 100 mm Petri dishes at 1×10^7 cells/dish. After attachment, the cells were treated with the selected compounds (10 and 50 μM) for 24 h and then incubated with H_2O_2 for another 2 h with the previous compounds removed.

2.7. Cell viability assay

PC12 cells were seeded in 96-well plates at 2×10^4 cells/well. After attachment, cells were incubated with tested compounds at 10 and 50 μM for 24 h. After incubation, cells were treated with 5 mg/mL MTT for 4 h at 37 °C. Then the media were carefully removed, the formazan crystals were dissolved in 150 μL of DMSO, the absorbance was measured at 570 nm on a plate reader. Controls utilized the same concentration of medium with DMSO alone. Cell viability was normalized as the percentage of control.

2.8. Western blot

Cytosolic and nuclear proteins were isolated with a Beyotime kit. The growth medium was removed after cell culture, and the cells were washed twice using 1 mL of PBS, added with 1 mL of PBS, and then scraped into centrifuge tubes on ice. The cells were centrifuged at 1200 × *g* for 5 min. The cells were added with Buffer A containing 1% PMSF on ice for 1 min, vortexed for 5 s, and then placed on ice for 20 min. Then, the cells were added with Buffer B, vortexed for 5 s, and then placed on ice for 1 min. The tubes were centrifuged at 12,000 × *g* for 15 min at 4 °C, added with Buffer N containing 1% PMSF on ice for 30 min, vortexed every 2–3 min, and then centrifuged again at 14,000 × *g* for 15 min at 4 °C. The protein concentration of the samples was detected by a Beyotime BCA protein assay kit, and all samples were stored at −80 °C for Western blot analysis. Western blot was performed using standard methods. In brief, protein samples (20–30 μg) were separated by SDS − PAGE and transferred onto PVDF membranes. The membranes were blocked in 5% milk − TBST and then incubated overnight at 4 °C in primary antibodies. Antibodies used included Nrf2 (Abcam), Histone H3 (Abcam), and β − actin (Abcam). Peroxidase − conjugated anti − mouse IgG (Abcam) or anti − rabbit IgG (Abcam) was used as the secondary antibody. Protein bands were visualized using ChemiScope series (Clinx Science Instruments, Shanghai, China). The gray value of protein bands was quantified using ImageJ (National Institutes of Health, Bethesda, Maryland, USA).

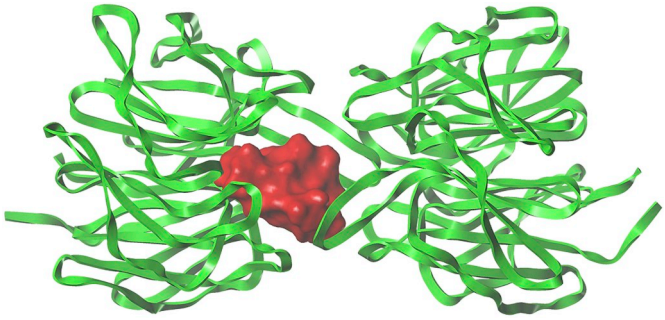

Fig. 1. The binding pocket of Keap1.
The green ribbon stands for the second structure of Keap1, the red region in the middle stands for the binding pocket that is easy to binding other compounds. (For interpretation of the references to colour in this figure legend, the reader is referred to the Web version of this article.)

2.9. Statistical analysis

One − way ANOVA with LSD analyses was performed using SPSS. All results were confirmed from three independent experiments. Data were expressed as the means ± standard error of the mean. Data were considered significantly different at $p < 0.05$.

3. Results

3.1. Docking calculations using SYBYL

Keap1 3D structure was prepared with SYBYL X 2.0, and the binding pocket, which easily interacted with other compounds, was obtained (Fig. 1). A library of 178 phytochemicals (Supplement Table 1) was prepared as mentioned in Section 2.1. The 178 phytochemicals were divided into 18 varieties according to their structural features: alkaloids, anthocyanins, carotenoids, chalcones, coumarins, flavanols, flavanones, flavones, flavonols, isoflavonoids, organosulfurs, phenolic acids, phenylethanoid glycosides, quinones, stibenes, terpenes, tocopherols, and others.

According to the rule of SYBYL X 2.0, C_Score shows hydrogen bonding, metal-ligand interaction, lipophilic contact, and rotational entropy, along with an intercept term. Total_Score shows the binding affinity between the ligand and protein. When Total_Score > 6, the ligand is considered as a candidate for further study, meanwhile the C_Score ≥4, the candidate is considered to be more promising. Here Average Total_Score is the average value of Total_Score of all the compounds with similar structural features. This value shows the binding affinity between the different classification of compounds and protein, was used to compare the binding affinity with Keap1 of 18 varieties of compounds. Docking calculation results (Table 1) showed that their binding affinity with Keap1 in descending order was shown and the Average Total_Score were as follows: phenylethanoid glycosides > tocopherols > flavones > flavanols > anthocyanins > flavonols > stibenes > flavanones > chalcones > carotenoids > isoflavonoids > phenolic acids > quinones > others > coumarins > terpenes > alkaloids > organosulfurs. These compounds could be divided into three groups, the high − total − score group (Average Total_Score > 6), the medium − total − score group (6 > Average

Table 2
24 compounds with potential interaction with Keap1.

Classification	PubChem CID	Name	Total_Score	C_score	Interactive Amino Acids
Anthocyanins	441688	Cyanidin 3,5-O-diglucoside	7.6511	3	Y334/S363/S508
Anthocyanins	6602304	Cyanidin 3-sambubioside	7.5814	4	S363/S602/S555/N414
Flavones	5280704	Apigenin 7-glucoside	6.0261	5	S363/S602
Flavones	5282150	Apigenin 7-O-neohesperidoside	6.7040	3	Y334/S363/S383/P384/S602
Flavones	12304093	Apigenin-7-O-glucoside	7.9129	4	Y334/S363
Flavones	9851181	Apigenin-7-O-rutinoside	8.0012	5	S363/P384/D385/N414/S602
Flavones	15559460	Luteolin-5-O-glucoside	6.6892	5	S363/N414/S602
Flavonols	5280805	Rutin	6.4747	4	S363/S508/S602
Flavonols	5318645	Isorhamnetin-3-O-glucoside	6.2842	4	S363/N414/S555/S602
Flavonols	17751019	Isorhamnetin-3-O-rutinoside	6.0438	3	S363/N414/S508/S602
Phenylethanoid glycosides	5281771	Echinacoside	9.3402	4	S363/P384/Y572
Phenylethanoid glycosides	16091519	Ternstroside A	8.9184	5	S363/N414/S508/S555/S602
Phenylethanoid glycosides	16091522	Ternstroside D	8.6565	5	S363/S602
Phenylethanoid glycosides	23958169	Isoforsythoside A	8.2334	4	S508/S555/S602
Phenylethanoid glycosides	6476333	Isoacteoside	8.1776	4	Y334/S555
Phenylethanoid glycosides	5281773	Forsythiaside A	8.1038	4	L365/I416/V463/S602
Phenylethanoid glycosides	16091521	Ternstroside C	8.0685	3	S363/N382/S383/D385/S508/Y572
Phenylethanoid glycosides	5281800	Acteoside	7.4971	5	Y334/S363/N382/N414/I416/L557/S602
Tocopherols	92094	δ-tocopherol	6.9734	3	S363
Tocopherols	14985	α-tocopherol	6.7759	3	Y572
Tocopherols	92729	γ-tocopherol	6.7727	3	S363
Tocopherols	5282347	α-tocotrienol	6.6725	4	None
Tocopherols	5282349	γ-tocotrienol	6.1956	2	S555
Tocopherols	6857447	β-tocopherol	6.0103	5	S363

D: aspartic acid; I, isoleucine; L, leucine; N, asparagine; P, proline; S, serine; V, valine; Y, tyrosine.

Total_Score > 3), and the low−total−score group (Average Total_Score < 3).

As shown in Table 2, 24 compounds showed strong binding affinity with Keap1 and most of them have C_Score ≥4. The interactive amino acids including Y334, S363, L365, N382, S383, P384, D385, N414, I416, V463, S508, S555, L557, Y572, S602. The 3D structure of binding mode between Keap1 and the 24 compounds above were shown in Supplement fig.1.

3.2. Effects of glycosides and oxygen molecules on binding affinity with Keap1

The 18 varieties of compounds were divided into two groups, the compounds containing glycosides (i.e., anthocyanins, flavanols, flavanones, flavones, flavonols, isoflavonoids, and phenylethanoid glycosides) and the compounds without glycosides (i.e., alkaloids, carotenoids, chalcones, coumarins, organosulfurs, phenolic acids, quinones, stibenes, terpenes, tocopherols, and others). The binding affinity with Keap1 of the compounds containing glycosides was better than the compounds without glycosides.

The number of glycosides was positively correlated with the binding affinity with Keap1. As shown in Table 3, phenylethanoid glycosides followed this typical pattern, and the binding affinity with Keap1 of phenylethanoid trisaccharides (ECH), phenylethanoid disaccharides (acteoside, isoacteoside), and phenylethanoid monosaccharides (salidroside) were in descending order. Compounds in Table 4 also showed better binding affinity with Keap1 when they existed in the form of glycosides. The more glycosides these compounds combine with, the higher score they obtained.

Meanwhile, the number of oxygen molecules was related to the binding affinity with Keap1. For example in Table 3, ternstroside A, ternstroside D, ternstroside C, ternstroside B, and ternstroside E were all phenylethanoid monosaccharides, and the only difference in their chemical formula was the number of oxygen molecules. Ternstroside A, ternstroside D, and ternstroside C contain 11 oxygens, whereas ternstroside B and ternstroside E contain 10 oxygens, which resulted in a significant difference in their binding affinity with Keap1: ternstroside A > ternstroside D > ternstroside C > ternstroside B > ternstroside E. The number of oxygen molecules was more sensitive than that of glycosides in predicting the binding affinity with Keap1.

3.3. QSAR between structure and their binding affinity with Keap1

In accordance with the method described in Section 2.5, the relationship between the structural parameters and the binding affinity was evaluated by 3D CoMFA studies in the QSAR module in SYBYL−X

Table 3
Molecular docking results of phenylethanoid glycosides.

Classification	PubChem CID	Name	Total_Score	C_score	Structural formula
Phenylethanoid trisaccharides	5281771	Echinacoside	9.3402	4	$C_{35}H_{46}O_{20}$
Phenylethanoid disaccharides	6476333	Isoacteoside	8.1776	4	$C_{29}H_{36}O_{15}$
	5281800	Acteoside	7.4971	5	$C_{29}H_{36}O_{15}$
Phenylethanoid monosaccharides	159278	Salidroside	5.1443	2	$C_{14}H_{20}O_7$
	16091519	Ternstroside A	8.9184	5	$C_{22}H_{26}O_{11}$
	16091522	Ternstroside D	8.6565	5	$C_{22}H_{26}O_{11}$
	16091521	Ternstroside C	8.0685	3	$C_{22}H_{26}O_{11}$
	16091520	Ternstroside B	5.8148	4	$C_{22}H_{26}O_{10}$
	16091523	Ternstroside E	5.7559	3	$C_{22}H_{26}O_{10}$

Table 4
Molecular docking results of compounds that existed in the form of glycosides.

Classification	PubChem CID	Name	Total_Score	C-score
Anthocyanins	128861	Cyanidin	4.1022	4
	441667	Cyanidin 3-O-glucoside	4.0842	4
	441674	Cyanidin 3-O-rutinoside	5.6498	4
	6602304	Cyanidin 3-sambubioside	7.5814	4
	441688	Cyanidin 3,5-O-diglucoside	7.6511	3
	128853	Delphinidin	3.6798	4
	443650	Delphinidin 3-O-glucoside	5.0364	4
	10196837	Delphinidin 3-sambubioside	5.9678	4
	159287	Malvidin	4.4472	4
	443652	Malvidin-3-glucoside	2.5509	3
	441765	Malvidin-3,5-diglucoside	4.6495	2
	440832	Pelargonidin	3.8220	4
	443648	Pelargonidin 3-O-glucoside	4.9631	4
	441773	Peonidin	4.2031	4
	443654	Peonidin 3-O-glucoside	5.8322	3
Flavonols	5280863	Kaempferol	3.4060	2
	5316673	Kaempferol 3-rhamnoside	3.3124	4
	5282155	Kaempferol 3-O-sophoroside	4.0080	2
	5282149	Kaempferol-3-O-galactoside	5.7907	3
	5318767	Kaempferol-3-O-rutinoside	5.5450	5
	5281672	Myricetin	4.9852	2
	5491408	Myricetin 3-galactoside	3.7234	5
	5352000	Myricetin 3-rhamnoside	5.8312	3
	5280343	Quercetin	4.0737	4
	5280804	Quercetin 3-glucoside	5.1733	3
	5282166	Quercetin 3-O-sophoroside	5.2882	4
	5487635	Quercetin 3-sambubioside	5.3734	4
	5280805	Quercetin 3-rutinoside	6.4747	4
	439533	Taxifolin	3.5443	3
	119258	Taxifolin 3-O-rhamnoside	5.2025	4
	14282775	Taxifolin 7-glucoside	5.5250	3
Flavanones	440735	Eriodictyol	3.6048	4
	11541786	Eriodictyol 7-O-sophoroside	4.0434	3
	22524386	Eriodictyol-7-O-glucoside	5.6722	4
	83489	Eriodictyol-7-O-rutinoside	4.6035	4
	932	Naringenin	3.2582	4
	25075	Naringenin 7-Rhamnoglucoside	5.2218	3
	92794	Naringenin-7-O-glucoside	5.2867	4
Flavones	5280443	Apigenin	3.7994	3
	5280704	Apigenin 7-glucoside	6.0261	5
	5282150	Apigenin 7-O-neohesperidoside	6.7040	3
	12304093	Apigenin-7-O-glucoside	7.9129	4
	9851181	Apigenin-7-O-rutinoside	8.0012	5
	5280445	Luteolin	4.0702	4
	5280637	Luteolin 7-glucoside	3.4014	4
	15559460	Luteolin-5-O-glucoside	6.6892	5

2.0. As shown in previous study, the $R^2 > 0.60$ was satisfactory. The R^2 between the experimental and predicted values was 0.975, which indicates that the structure was a key element in binding to Keap1. The cross−validation analysis, wherein 20 compounds were randomly selected by the system, showed a good relationship between the structural parameters and the binding affinity. The plot of the actual versus predicted Total_Score values is shown in Fig. 2.

3.4. Nrf2 activation effects of selected compounds

In the results above, 178 phytochemicals were divided into three groups depending on their binding affinity with Keap1. To evaluate their activation effect on Nrf2, 11 different compounds including C3S, L5G, RUT, API, KAEM, αT, COP, MAG, PIP, EA, and ECH from high−, medium−, and low−total−score groups were selected for further studied on a cell model.

The cytotoxicity assays was conducted at 10, 50, 100 μM, L5G, αT, and KAEM significantly reduced cell viability at 100 μM (Fig. 3). So the compounds were tested at 10 or 50 μM in further study.

As shown in Fig. 4, the Nrf2 expression level in the nucleus increased after treatment with C3S, L5G, RUT, API, KAEM, αT, COP, MAG, PIP, EA, and ECH at 10 or 50 μM. Results of Western blot and gray density analyses showed that all of these tested compounds exerted no significant influence on Nrf2 expression in the cytosol (Fig. 4A and B) ($p > 0.05$). C3S, L5G, RUT, αT, and ECH whose Total_Score were > 6 increased Nrf2 expression in the nucleus (Fig. 4C and D) ($p < 0.01$), and their effect on Nrf2 activation in descending order is as follows: C3S (46.54%, 61.80%) > αT (51.99%, 59.54%) > L5G (26.47%, 42.46%) > ECH (12.51%, 30.19%) > RUT (16.69%, 18.21%). This order was consistent with their Total_Score value (except ECH). Meanwhile, API and KAEM from the medium−total−score group and COP, MAG, and PIP from the low−total−score group showed no effect on Nrf2 activation (except PIP at 50 μM). The results above indicated that the compounds showing potential binding affinity (Total_Score > 6, C_score ≥ 4) with the Nrf2 binding site in Keap l can activate Nrf2 under oxidative stress.

4. Discussion

In the present study, 178 phytochemicals were investigated to make sure whether they can effectively activate the transcription factor Nrf2 using molecular docking methods. The main findings of this study were as follows: (1) Structure of the compounds determined their inhibitory effect on the Keap1–Nrf2 protein–protein interaction. Compounds with abundant oxygen or glycosides effectively inhibited the Keap1–Nrf2 interaction. (2) The steric/acceptor/hydrophobic contribution instead of the electrostatic/donor contribution was the predominant element affecting the binding affinity. (3) Compounds with higher Total_Score (Total_Score > 6) in binding affinity with Keap1 showed significantly positive effects on the nuclear translocation of Nrf2 in the H_2O_2−induced oxidative−injured cell model.

Molecular docking is a very powerful technique for screening large numbers of new compounds as active drug candidates, and this technique has been successfully used in the discovery of antimicrobial (Shen et al., 2010), Alzheimer's disease related cyclophilin D inhibitors (Valasani et al., 2014), human coronavirus nucleocapsid protein inhibitors (Chang et al., 2016). Previous studies paid great attention to antioxidants and Nrf2 activators; however, few of these studies systematically screened Nrf2 activators from known antioxidants. Wu et al. (2014) utilized AREc32 cells that contain a luciferase gene under the control of antioxidant response element promoters to screen Nrf2 activators. In this study, 178 phytochemicals were selected from the literature and directly explored whether they can activate Nrf2 by inhibiting the Keap1–Nrf2 protein–protein interaction using the molecular docking method. With the help of the software, 24 candidates were obtained, and the results showed that the number of glycosides and oxygen positively correlated with the binding affinity of compounds with Keap1. The procedure above was easy to operate and time saving.

Further study showed that the C3S, L5G, RUT, αT, and ECH from the 24 candidates can significantly increase the Nrf2 level in the nucleus. Several studies have reported about the antioxidant effects of αT

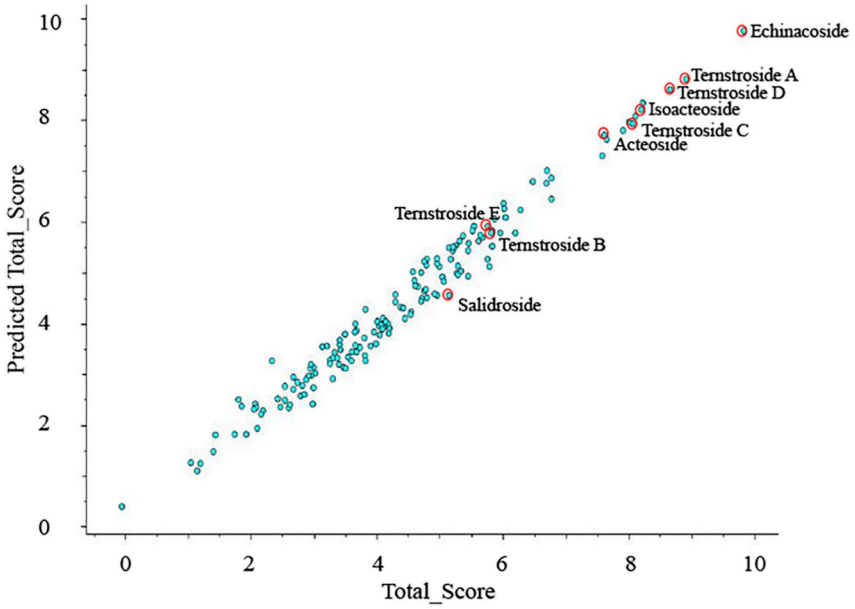

Fig. 2. Graph between actual Total_Score and predicted. Total_ScoreThe X axe: Total_Score is the true value from molecular docking. The Y axe: Predicted Total_Score is the virtual value from 3D CoMFA studies the blue spots stand for tested compounds, the red circle stand for phenylethanoid glycosides. (For interpretation of the references to colour in this figure legend, the reader is referred to the Web version of this article.)

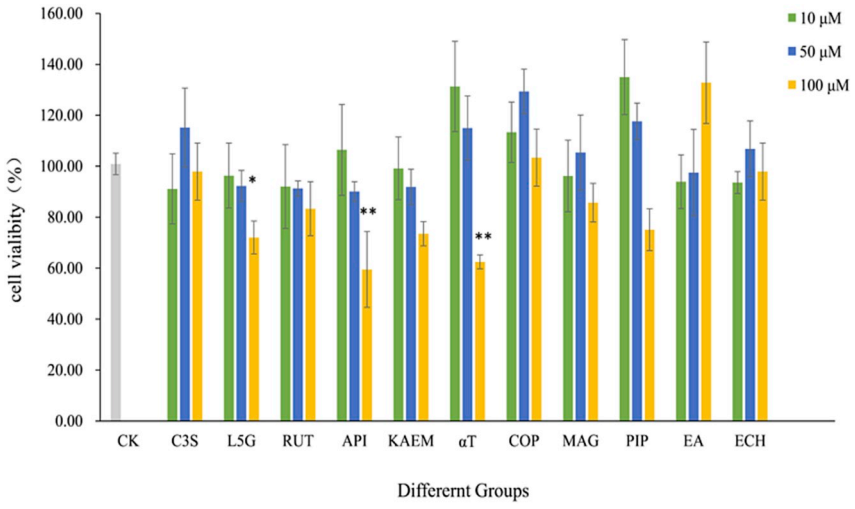

Fig. 3. Cytotoxicity study of tested 11 compounds on PC12 cells.
Cell viability was detected by MTT assay. CK: control group, C3S: cyanidin 3-sambubioside treated group, L5G: luteolin-5-O-glucoside treated group, RUT: rutin treated group, API: apigenin treated group, KAEM: kaempferol treated group, αT: α-tocopherol treated group, COP: coptisine treated group, MAG: magnoflorine treated group, PIP: piperine treated group, EA: ellagic acid treated group, ECH: echinacoside treated group. $\#p < 0.05$, versus control group, $\#\#p < 0.01$, versus control group.

(Niki, 2014) and ECH (And and Kitts, 2000). Masoudi et al. (2014) reported that αT activates the transcription factor Nrf2 in neuronal cells and that ECH is a representative antioxidant compound in Herba Cistanches (Tu et al., 1997). C3S (Cheng et al., 2009) was subjected to DPPH scavenging activities, AOP, and reducing power assessments; a dose−dependent antioxidant activity was observed. L5G (Jung et al., 2017) in Korean milk thistle strongly protects t−BHP−treated HepG2 cells from oxidative damage, and these protective effects might be attributed to Nrf2 activation. RUT (Tian et al., 2015) significantly attenuates oxidative stress and upregulates Nrf2 expression in a rat model. Previous studies are consistent with our results.

The 24 candidates bind with the special amino acids on Keap1, such as Ser363, Ser508, Ser555 and Ser602, which have been reported to be the key amino acids in the structure of the Keap1−Nrf2 interface (Lo et al., 2014). The results indicated that the compounds with high binding affinity with Keap1 could directly inhibit Keap1−Nrf2 protein−protein interaction as Nrf2 activators.

5. Conclusion

Antioxidants have the potential to activate Nrf2 by inhibiting the Keap1−Nrf2 protein−protein interaction, and the effect is largely determined by their structures. Compounds with abundant oxygen or glycosides can inhibit the Keap1−Nrf2 interaction more effectively and phenylethanoid glycosides showed the best effect among the 18 varieties. High−total−score group (Total_Score > 6) show significant effects on the nuclear translocation of Nrf2 in H_2O_2−induced oxidative−injured cell model. These results may provide a new method for discovering Nrf2 activators that interfere with Keap1−Nrf2 protein−protein interaction.

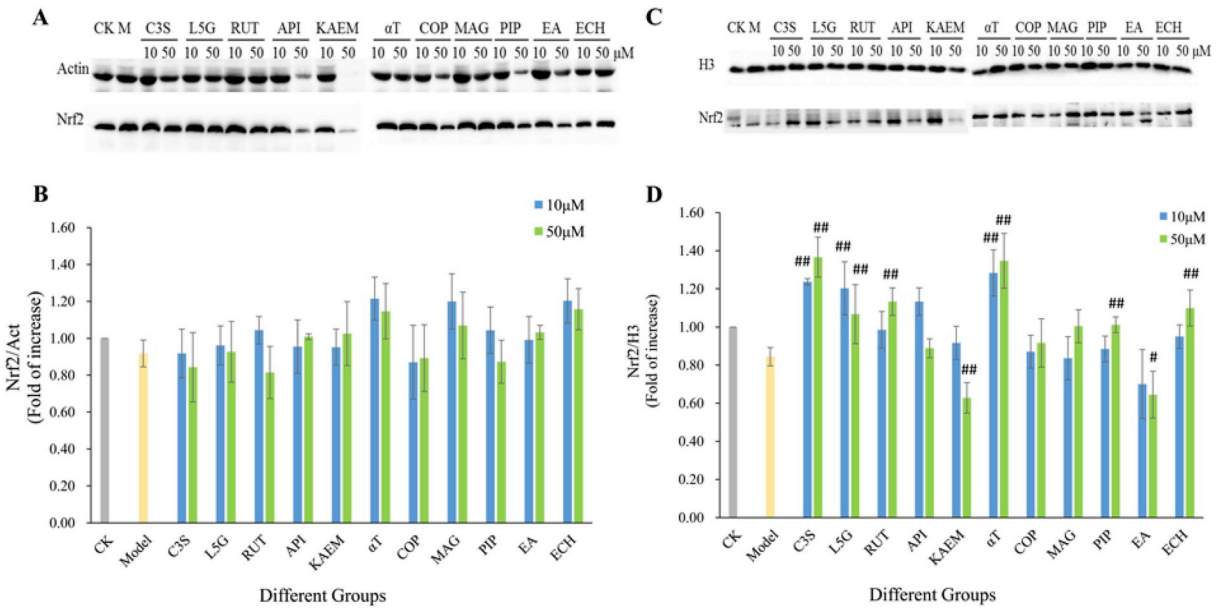

Fig. 4. The influence of tested 11 compounds on Nrf2 expression both in cytoplasm and nucleus.
PC12 cells were incubated with tested compounds (10 μM 50 μM) for 24 h, and then incubated with 200 μM H_2O_2 for another 2 h after the previous compounds removed. (A) The expression of Nrf2 protein in cytoplasm was detected by immunoblotting using specific antibody. β-Actin was used as loading control. (B) The quantitative densitometric analyses of Nrf2 protein in cytoplasm. (C) The expression of Nrf2 protein in nucleus was detected by immunoblotting using specific antibody. Histones H3 was used as loading control. (D) The quantitative densitometric analyses of Nrf2 protein in nucleus. All data are expressed as means ± SD and represent three independent experiments. CK: control group, Model: H_2O_2 treated group, C3S: cyanidin 3-sambubioside treated group, L5G: luteolin-5-O-glucoside treated group, RUT: rutin treated group, API: apigenin treated group, KAEM: kaempferol treated group, αT: α-tocopherol treated group, COP: coptisine treated group, MAG: magnoflorine treated group, PIP: piperine treated group, EA: ellagic acid treated group, ECH: echinacoside treated group. α − Tocopherol was used as a positive control. $\#p < 0.05$, versus H_2O_2 treated group, $\#\#p < 0.01$, versus H_2O_2 treated group.

Declaration of interests

The authors declare that they have no known competing financial interests or personal relationships that could have appeared to influence the work reported in this paper.

Author contributions

Baiyi Lu and Maiquan Li designed the study. Maiquan Li performed the laboratory work, data analysis and wrote the paper. All authors revised the manuscript.

Conflicts of interest

The authors hereby declare no conflict of interest.

Acknowledgments

This study was supported by the Zhejiang Provincial Major R & D Program of China (No. 2019C02070), the Zhejiang Provincial Natural Science Foundation of China (no. R15C200002) and the Special Project of Agricultural Product Quality Safety Risk Assessment (no. GJFP2019043), Ministry of Agriculture and Rural Affairs of China.

Appendix A. Supplementary data

Supplementary data to this article can be found online at https://doi.org/10.1016/j.fct.2019.110758.

References

Anatoliotakis, N., Deftereos, S., Bouras, G., Giannopoulos, G., Tsounis, D., Angelidis, C., Kaoukis, A., Stefanadis, C., 2013. Myeloperoxidase: expressing inflammation and oxidative stress in cardiovascular disease. Curr. Top. Med. Chem. 13 (2), 115–138.
H, K., Koppula, S., Kim, I.S., More, S.V., Kim, B.W., Choi, D.K., 2012. Nuclear factor erythroid 2 - related factor 2 signaling in Parkinson disease: a promising multi therapeutic target against oxidative stress, neuroinflammation and cell death. CNS Neurol. Disord. - Drug Targets 11 (8), 1015–1029.
C.H, Kitts, D.D., 2000. Studies on the antioxidant activity of echinacea root extract. J. Agric. Food Chem. 48 (5), 1466.
Chang, C.K., Jeyachandran, S., Hu, N.J., Liu, C.L., Lin, S.Y., Wang, Y.S., Chang, Y.M., Hou, M.H., 2016. Structure-based virtual screening and experimental validation of the discovery of inhibitors targeted towards the human coronavirus nucleocapsid protein. Mol. Biosyst. 12 (1), 59.
Cheng, J.C., Kan, L.S., Chen, J.T., Chen, L.G., Lu, H.C., Lin, S.M., Wang, S.H., Yang, K.H., Chiou, R.Y.Y., 2009. Detection of cyanidin in different-colored peanut testae and identification of peanut cyanidin 3-sambubioside. J. Agric. Food Chem. 57 (19), 8805–8811.
Cramer, R.D., Patterson, D.E., Bunce, J.D., 1988. Comparative molecular field analysis (CoMFA). 1. Effect of shape on binding of steroids to carrier proteins. J. Am. Chem. Soc. 110 (18), 5959–5967.
Dhakshinamoorthy, S., Jaiswal, A., 2001. Functional characterization and role of Nrf2 in ARE-mediated expression and antioxidant induction of NAD(P)H:Quinone oxidoreductase 1 gene. Oncogene 20 (29), 3906–3917.
Emerit, J., Edeas, M., Bricaire, F., 2004. Neurodegenerative diseases and oxidative stress. Biomed. Pharmacother. 58 (1), 39.
Ferreira, L.G., Dos Santos, R.N., Oliva, G., Andricopulo, A.D., 2015. Molecular docking and structure-based drug design strategies. Molecules 20, 13384.
Fiedor, J., Burda, K., 2014. Potential role of carotenoids as antioxidants in human Health and disease. Nutrients 6 (2), 466.
Ji, L.L., Sheng, Y.C., Zheng, Z.Y., Shi, L., Wang, Z.T., 2015. The Involvement of p62-Keap1-Nrf2 antioxidative signaling pathway and JNK in the protection of natural flavonoid quercetin against hepatotoxicity. Free Radical Biology & Medicine 85, 12–23.
Jung, H.A., Abdul, Q.A., Byun, J.S., Joung, E.J., Gwon, W.G., Lee, M.S., Kim, H.R., Choi, J.S., 2017. Protective effects of flavonoids isolated from Korean milk thistle Cirsium japonicum var. maackii (Maxim.) Matsum on tert-butyl hydroperoxide-induced hepatotoxicity in HepG2 cells. J. Ethnopharmacol. 209, 62.
Kiokias, S., Varzakas, T., Oreopoulou, V., 2008. In vitro activity of vitamins, flavonoids, and natural phenolic antioxidants against the oxidative deterioration of oil-based systems. Crit. Rev. Food Sci. Nutr. 48 (1), 78–93.
Kumar, H., More, S.V., Han, S.D., Choi, J.Y., Choi, D.K., 2012. Promising therapeutics with natural bioactive compounds for improving learning and memory–a review of randomized trials. Molecules 17 (9), 10503.
Lo, S.C., Li, X., Henzl, M.T., Beamer, L.J., Hannink, M., 2014. Structure of the Keap1:Nrf2 interface provides mechanistic insight into Nrf2 signaling. EMBO J. 25 (15), 3605–3617.
Magesh, S., Chen, Y., Hu, L., 2012. Small molecule modulators of keap1-nrf2-ARE pathway as potential preventive and therapeutic agents. Med. Res. Rev. 32 (4), 687–726.
Masoudi, S., Ploen, D., Kunz, K., Hildt, E., 2014. The adjuvant component α-tocopherol

triggers via modulation of Nrf2 the expression and turnover of hypocretin in vitro and its implication to the development of narcolepsy. Vaccine 32 (25), 2980–2988.
Mcmahon, M., Itoh, K., Yamamoto, M., Hayes, J.D., 2003. Keap1-dependent proteasomal degradation of transcription factor Nrf2 contributes to the negative regulation of antioxidant response element-driven gene expression. J. Biol. Chem. 278 (24), 21592–21600.
Meng, X.Y., Zhang, H.X., Mezei, M., Cui, M., 2011. Molecular docking: a powerful approach for structure-based drug discovery. Curr. Comput. Aided Drug Des. 7 (2), 146–157.
Niki, E., 2014. Role of vitamin E as a lipid-soluble peroxyl radical scavenger: in vitro and in vivo evidence. Free Radical Biol. Med. 66 (2), 3.
Pang, C., Zheng, Z., Liang, S., Sheng, Y., Wei, H., Wang, Z., Ji, L., 2016. Caffeic acid prevents acetaminophen-induced liver injury by activating the Keap1-Nrf2 antioxidative defense system. Free Radical Biol. Med. 91, 236.
Rehman, S., Khan, H., 2017. Advances in antioxidant potential of natural alkaloids. Curr. Bioact. Compd. 13 (2), 101–108.
Reuter, S., Gupta, S.C., Chaturvedi, M.M., Aggarwal, B.B., 2010. Oxidative stress, inflammation, and cancer: how are they linked? Free Radical Biol. Med. 49 (11), 1603–1616.
Shen, Y., Liu, J., Estiu, G., Isin, B., Ahn, Y.Y., Lee, D.S., Barabási, A.L., Kapatral, V., Wiest, O., Oltvai, Z.N., 2010. Blueprint for antimicrobial hit discovery targeting metabolic networks. Proc. Natl. Acad. Sci. U. S. A 107 (3), 1082.
Singh, S.K., Dessalew, N., Bharatam, P.V., 2007. 3D-QSAR CoMFA study on oxindole derivatives as cyclin dependent kinase 1 (CDK1) and cyclin dependent kinase 2 (CDK2) inhibitors. Medicinal Chemistry 3, 75.
Steinmetz, K.A., Potter, J.D., 1996. Vegetables, fruit, and cancer prevention: a review. J. Am. Diet. Assoc. 96 (10), 1027–1039.
Tian, R., Yang, W., Xue, Q., Gao, L., Huo, J., Ren, D., Chen, X., 2015. Rutin ameliorates diabetic neuropathy by lowering plasma glucose and decreasing oxidative stress via Nrf2 signaling pathway in rats. Eur. J. Pharmacol. 771, 84–92.
Tu, P.F., Wang, B., Deyama, T., Zhang, Z.G., Lou, Z.C., 1997. Analysis of phenylethanoid glycosides of Herba cistanchis by RP-HPLC. Yao xue xue bao = Acta pharmaceutica Sinica 32 (4), 294.
Valasani, K.R., Vangavaragu, J.R., Day, V.W., Yan, S.D., 2014. Structure based design, synthesis, pharmacophore Modeling,Virtual screening, and molecular docking studies for identificationof novel cyclophilin D inhibitors. J. Chem. Inf. Model. 54 (3), 902.
Wu, K.C., Mcdonald, P.R., Liu, J., Klaassen, C.D., 2014. Screening of natural compounds as activators of the keap1-nrf2 pathway. Planta Med. 80 (1), 97.
Zhang, N., Zhong, R., 2010. Docking and 3D-QSAR studies of 7-hydroxycoumarin derivatives as CK2 inhibitors. European Journal of Medicinal Chemistry 45, 292.